

Prediction of Solar Cycle 25

Leif Svalgaard^{1*}

¹W.W. Hansen Experimental Physics Laboratory, Stanford University
Cypress Hall, C3, 466 Via Ortega, Stanford, CA 94305-4085

*Corresponding author: Leif Svalgaard (leif@leif.org)

ABSTRACT

Prediction of solar cycle is an important goal of Solar Physics both because it serves as a touchstone for our understanding of the sun and also because of its societal value for a space faring civilization. The task is difficult and progress is slow. Schatten et al. (1978) suggested that the magnitude of the magnetic field in the polar regions of the sun near solar minimum could serve as a *precursor* for the evolution and amplitude of the following solar cycle. Since then, this idea has been the foundation of somewhat successful predictions of the size of the last four cycles, especially of the unexpectedly weak solar cycle 24 (“the weakest in 100 years”). Direct measurements of the polar magnetic fields are available since the 1970s and we have just passed the solar minimum prior to solar cycle 25, so a further test of the polar field precursor method is now possible. The predicted size of the new cycle 25 is 128 ± 10 (on the new sunspot number version 2 scale), slightly larger than the previous cycle.

Keywords: Solar Cycle Prediction / Polar Magnetic Fields / Precursor Method / SC25

1. Introduction

The solar cycle is driven by a self-exciting dynamo that converts poloidal magnetic fields into azimuthal or toroidal fields erupting as solar active regions and sunspots (e.g. Charbonneau (2020)). Prediction of solar activity is important for, among other things, planning and management of space missions, communications, and power transmission. As Max Waldmeier suggested, solar cycle shapes seem to form a family of curves well characterized by a single parameter: SN_{Max} , the maximum smoothed monthly sunspot number (Waldmeier, 1955; Hathaway et al., 1994). Predicting the amplitude, shape, and duration of the next cycle thus concentrates on predicting SN_{Max} for the cycle. Our current knowledge of the sun is insufficient to predict solar activity directly from physical theory. The many empirical prediction methods that have been tried instead fall in two broad categories (Pesnell, 2016, 2018, 2020; NOAA, 2019): statistical methods and precursor methods. The former assume that the centuries-long time-series of sunspot numbers carries information about the underlying physics that can be exploited for forecasting. Precursor methods assume that some properties of the recent cycles, perhaps only part of the most recent, have predictive power for the next. At any rate “The predictions must be believable even if they aren’t physically correct” (Pesnell, 2020).

2. Method

Schatten, Scherrer, Svalgaard, and Wilcox (Schatten et al., 1978) suggested on assumed physical grounds (the Babcock-Leighton model of the solar dynamo) that the magnetic field in the polar regions near minimum would be a precursor proxy for the amount of sunspot activity in the following cycle, serving as a ‘seed’ for the dynamo when advected into the solar interior. Schatten and colleagues obtained reasonable success using a (slightly modified) polar field precursor for prediction of Cycles 21 through 24 (Schatten, 2005), while Svalgaard et al. (2005)

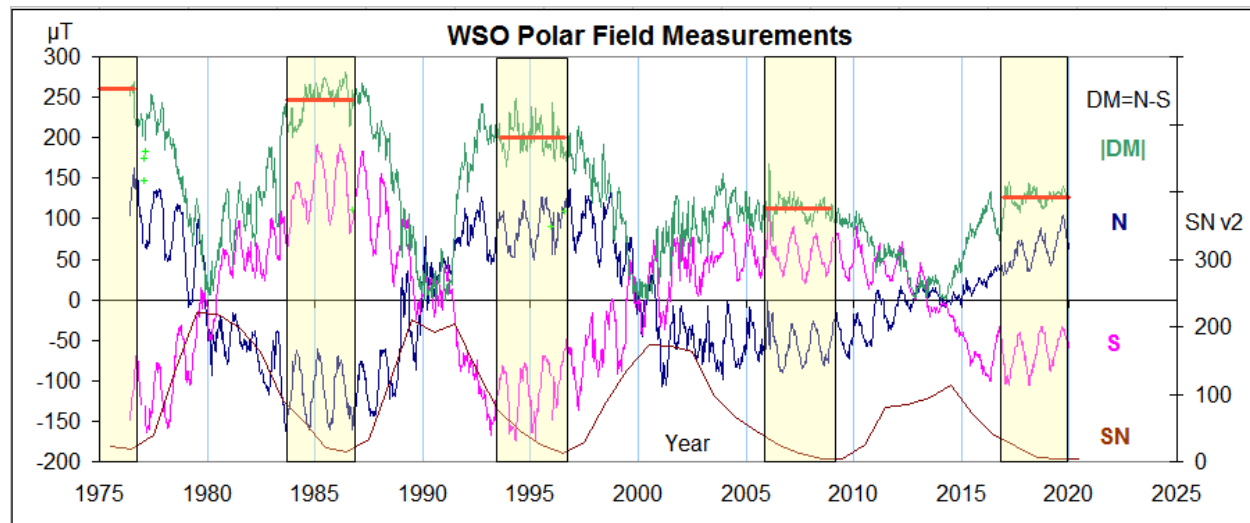
43 suggested using the average polar fields during the three-year interval preceding solar minimum
 44 as the precursor value to regress against the amplitude of the following cycle. The present paper
 45 aims at predicting Solar Cycle 25 utilizing the polar magnetic field data obtained at WSO using
 46 essentially the same methodology as Svalgaard et al. (2005). With solar minimum just passed at
 47 the end of 2019 (NASA, 2020) the present is now right for application of the method.

48 3. Data

49 The sun's magnetic field near the poles has been measured regularly with the required sensitivity
 50 at Mount Wilson Observatory (MWO (Ulrich et al., 2002), since 1967) and at Wilcox Solar
 51 Observatory (WSO (Svalgaard et al., 1978), since 1976). Details about the observations can be
 52 found in Svalgaard et al. (2005) where the data were used to (successfully) predict Solar Cycle
 53 24. The polar magnetic field data curated by Todd Hoeksema can be obtained from the WSO
 54 website at <http://wso.stanford.edu/Polar.html>. The measurements are actually of the line-of-sight
 55 magnetic flux density over a 3' aperture and suffer from magnetograph saturation (diminished by
 56 a factor of 1.8 (Svalgaard et al., 1978)) and 'filling factor' dilution from kiloGauss elements to
 57 much weaker (by three orders of magnitude) area averages, but we shall for convenience simply
 58 refer to them as 'the field' expressed in 'pseudo' microTesla ($100 \mu\text{T} = 1 \text{ Gauss}$), because only
 59 relative values are used. Because of projection effects near the limb of the strongly concentrated
 60 'topknot' vertical polar 'fields', the reported values vary by about a factor of two through the
 61 year, already noted by the Babcocks (1955) when the field was first definitively observed back in
 62 the early 1950s, and substantiated for modern data by Svalgaard et al. (1978, 2005).

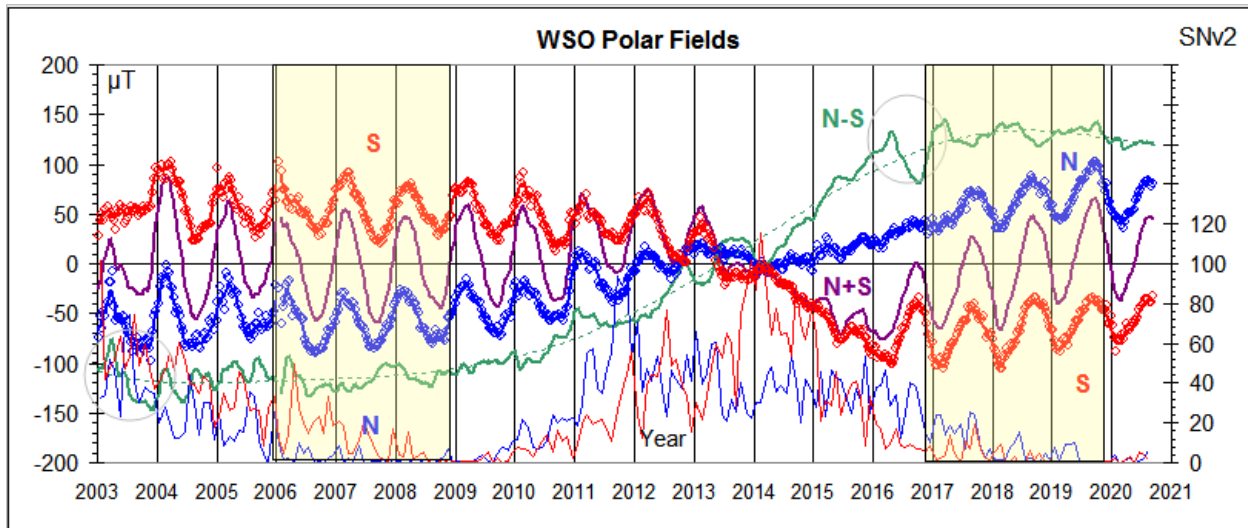
63 3.1 The regular variation of the observed polar cap fields

64 The main feature of the method proposed in Svalgaard et al. (2005) was to suggest that once
 65 stable polar fields had built up some time after the polar field reversal(s), the resulting average
 66 dipole moment (measured as the absolute value of the difference between the two polar caps
 67 fields) would be a proxy for the seed field of a dynamo producing the next solar cycle. A distinct
 68 signature of when stable polar fields were established would be the appearance of the regular
 69 annual modulation of the observed field beginning after the irregular variations during the time
 70 of reversals at or about the time of sunspot maximum, as only a stable (or, at least, slowly
 71 varying) polar cap field would exhibit a regular annual variation in phase with the heliographic
 72 latitude of the observer, Figure 1:



74 **Figure 1.** WSO polar field measurements: 30-day averages of north polar aperture line-of-
 75 sight fields (dark blue) and of south polar fields (pink), both sampled every ten days. The
 76 (unsigned) ‘Dipole Moment’ is defined as $DM = |(\text{field(North)} - \text{field(South)})|$, green curve.
 77 The average values for intervals (light yellow shading) of three years before solar minima
 78 (yearly values of the sunspot number shown by the brown curve) are marked by red horizontal
 79 lines. During these intervals the annual modulation is clearly seen in the polar fields. As the
 80 modulations are opposite between hemispheres they cancel out for the Dipole Moment.

81 As the transition from Cycle 24 to Cycle 25 is somewhat unusual (e.g. highly hemispherically
 82 asymmetrical) it is of interest to show it in more detail, Figure 2:



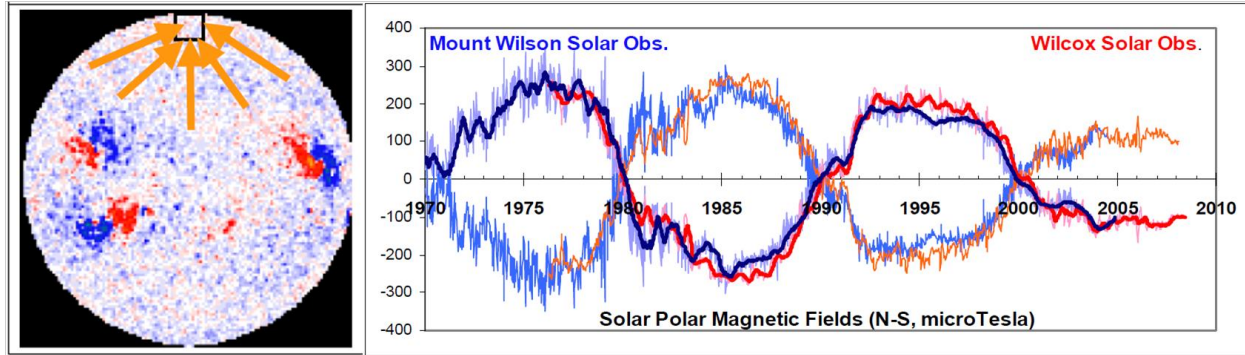
83 **Figure 2.** WSO polar field measurement details: 30-day averages of the north polar aperture
 84 line-of-sight fields (blue) and of the south polar fields (red), both sampled every ten days.
 85 During intervals (light yellow shading) of three years before solar minima the annual
 86 modulation of the polar fields ($N+S$, violet curve) is strong and stable. As the modulations are
 87 opposite between hemispheres they cancel out for the signed Dipole Moment ($N-S$, green curve).
 88 The sunspot numbers (SN v2) separately for each hemisphere are shown as thin blue
 89 (North) and red (South) curves at the bottom of the Figure.

90 After the reversal in 2014 a strong ‘surge’ of solar activity in the southern hemisphere resulted in
 91 the build-up of significant field in the southern polar cap about a year and a half later
 92 (commensurate with the time it takes the meridional circulation to carry the flux to the polar cap)
 93 and initiating the visibility of the annual modulation. Similarly, a surge in the northern
 94 hemisphere in 2011 caused the early reversal of the north polar field after a similar delay. The
 95 association of surges of activity with subsequent polar field reversals is a common feature of the
 96 magnetic evolution of solar cycles (Svalgaard & Kamide, 2013; Shukuya & Kusano, 2017) and
 97 is useful in interpreting the data.

98 3.2 The effect of scattered light

99 During 1976-1977 the WSO measurements were contaminated by scattered light (Scherrer et al.,
 100 1980). Dirty optics and poor atmospheric conditions cause light from mixed polarity areas to be
 101 scattered into the polar aperture, diluting the measured polar field. Making the optics dirty on
 102 purpose (Svalgaard & Schatten, 2008) showed that each percent of scattered light (measured 1

104 arc minute off the limb) decreased the measured polar field by 3.5%. Before 1978 (after that, we
 105 kept the optics clean) scattered light at WSO was large and highly variable, but was typically
 106 about 5% on average, causing a decrease of the measured field by about 18%. Correcting for this
 107 brings WSO to agree with (suitably scaled) MWO (Svalgaard et al., 2005), Figure 3:



108
 109 **Figure 3.** (Left) Scattering of light into the polar aperture. (Right) Time variation of the solar
 110 magnetic axial dipole moment (expressed as the difference (N-S) between the polar fields in
 111 the North (N) and in the South (S)). Also plotted is the difference between S and N (S-N).
 112 MWO data are shown with bluish colors. WSO data are shown with reddish colors. Heavy
 113 lines show 12-month running mean values of the N-S difference. Adapted from Svalgaard &
 114 Schatten (2008).

115 We do not have measurements of DM at WSO for times before the minimum in 1976, but only
 116 for just after the minimum when the fields have already begun their decline due to new flux
 117 arriving at the polar caps from lower-latitude decaying sunspots from the growing Cycle 21.
 118 Comparing the decline with similar declines for the other cycles allows us to ‘guesstimate’ a
 119 likely DM for the years prior to the minimum between Cycles 20 and 21. This (somewhat
 120 uncertain) value has been entered in Table 1.

121 3.3 Parameters used for the prediction

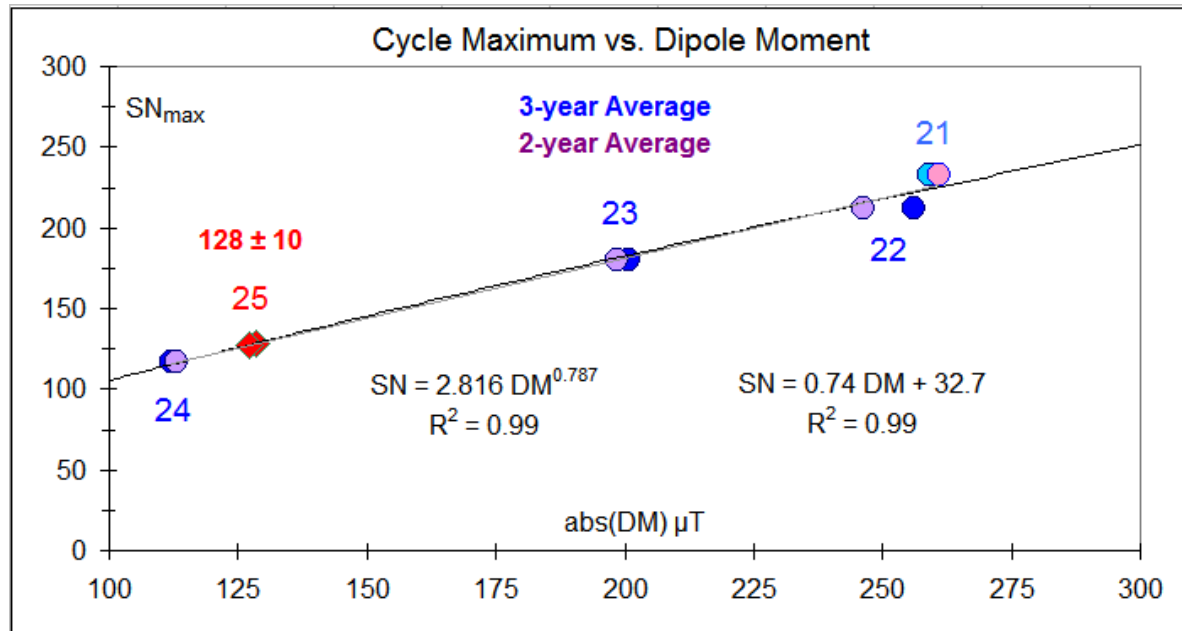
122 In Table 1 we collect the relevant parameters and data values. In addition, we calculate the
 123 predicted values of SN_{Max} using two regression relationships (see Figure 4), one linear and the
 124 other a power law, not having any reason to prefer one over the other (or any other fitting
 125 function), and take their average result as our prediction. All parameters have uncertainties (not
 126 stated), but since the greatest (and unknown) uncertainties are in the assumptions and in the
 127 unknown details of the internal plasma flows, we refrain from the numerology of combining
 128 knowns with unknowns, but see Section 4.1.

129 **Table 1.** WSO Measured (or *estimated*) dipole moments (column 3) for the minima before
 130 Cycles 21 through 25 computed as the (absolute) difference between the reported fields in the
 131 polar caps (above latitude 55°) averaged (column 2) over three years before the minima in the
 132 top half of the Table and over two years before the minima in the bottom half. Values that are
 133 particularly uncertain are entered in *italics*. Column 4: The observed maximum values of the
 134 smoothed monthly sunspot numbers (version 2; Clette et al. (2014)) for each cycle. Columns
 135 5 and 6: Sunspot number calculated from the DM using the relationships derived from the
 136 regressions shown in Figure 4 below. Column 7: The predicted SN_{Max} is taken as the average
 137 of columns 5 and 6. Column 8: The percentage error of the prediction ($\Delta\% = |col.7-$
 138 $col.4|/col.4 \times 100$). Column 9: The time of solar minimum before each cycle.

Before Cycle	Years Averaged	$ \text{DM} \mu\text{T}$	$\text{SN}_{\text{Max}} \text{ v2 Obs.}$	$\text{SN}_{\text{Max}} \text{ Linear}$	$\text{SN}_{\text{Max}} \text{ Power}$	$\text{SN}_{\text{Max}} \text{ Predicted}$	$\Delta\% \text{ Error}$	Time Min.
21	3	260	233	225	224	225	3.6	1976.4
22	3	256	212	222	221	222	4.4	1986.7
23	3	200	180	181	182	181	0.5	1996.6
24	3	112	116	116	115	116	0.8	2008.9
25	3	129		128	129	128	2.3	2019.9
21	2	260	233	225	224	225	3.6	1976.4
22	2	246	212	215	215	215	1.1	1986.7
23	2	199	180	180	182	181	0.5	1996.6
24	2	113	116	117	116	116	0.0	2008.9
25	2	127		127	128	127	1.3	2019.9
Result				0.74DM+32.7	2.816DM ^{0.787}	128	1.8	

139 4. Results

140 Using the data in Table 1 we regress SN_{Max} against the DM for Cycles 21-24, using both 3-year
 141 and 2-year averages of DM prior to solar minima (Figure 4). The two regression fits have (likely
 142 fortuitously) very high coefficients of determination R^2 of 0.99. As elaborated in Table 1, the
 143 resulting predicted maximum SN comes to 128.



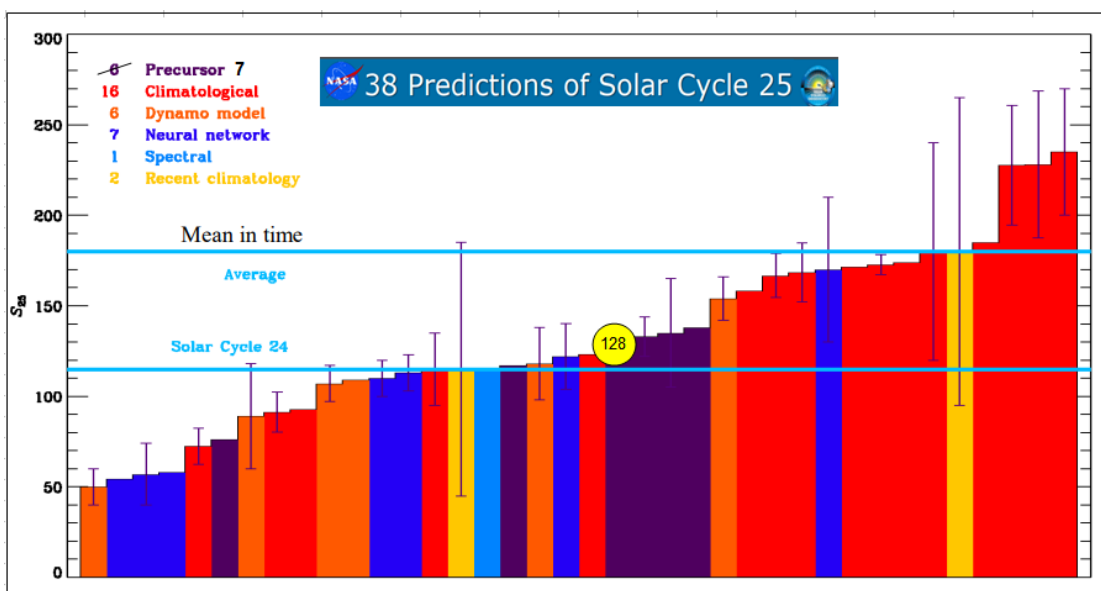
144 **Figure 4.** Smoothed monthly maximum sunspot number, SN_{Max} , for cycles 21-24 regressed
 145 against the (absolute) Dipole Moment averaged over three years before solar minimum (blue
 146 symbols) and over two years (violet symbols). Symbols of lighter shade are used for the more
 147 uncertain Cycle 21. Where symbols completely cover each other, they have been offset
 148 slightly for display purposes. The prediction for Cycle 25 is shown with red diamonds.

149 4.1 Estimation of likely prediction error

150 If predicting the solar cycle maximum is difficult, assigning an uncertainty to the prediction is
 151 fraught with even more difficulty. If the ‘error band’ is too wide, the prediction is useless and not
 152 actionable. If it is too narrow, the prediction is ‘too good to be true’. As Pesnell (2020) pointed
 153 out, the prediction must be ‘believable’. People who use the predictions (such as NASA’s Flight
 154 Dynamics Group) require error bars. The errors are then used in Monte Carlo models of the
 155 satellite drag over the next sunspot cycle (Pesnell 2020, personal communication). The only real
 156 way to estimate the error of a prediction method is to compare the (past) predictions to what was
 157 actually observed. The predictions of Svalgaard et al. (2005) and Schatten (2005) were off by 6%
 158 overall, several times larger than the (formal) error of 1.8% reported in Table 1 using the recent
 159 regressions. On top of that, there is uncertainty in how well the sunspot number represents actual
 160 solar activity. The SILSO data product lists a typical standard deviation of cycle-maximum of the
 161 sunspot number of 6%, for a combined ‘error’ of 8.5% or 11 sunspot units for a SN of 128. We
 162 shall round that to 10 SN-units as even the unit digit is uncertain.

163 **5. Conclusion**

164 That solar cycle prediction is still in its infancy is borne out by the extreme range of predictions
 165 of Cycle 25 (Pesnell, 2020; see Figure 5 below) indicating that we have not made much progress
 166 since predictions were made of Cycle 24 (Pesnell, 2016), which showed a similar spread (from
 167 half to double of actual value observed). With the wide spread (from 50 (Kitiashvili, 2020) to
 168 233 (McIntosh et al., 2020)), someone or even several ones are bound to be ‘correct’, regardless
 169 of the possible correctness of the method used. The many non-overlapping error bars illustrate
 170 the folly of even assigning error bars to the predictions or, at least, to believe in them. Our
 171 prediction is shown by the yellow circle in the middle of the plot, its diameter being its error bar.
 172



173 **Figure 5.** The 38 predictions of Solar Cycle 25 that had been registered by January 2020
 174 (Adapted after Pesnell (2020), with permission). Our prediction (128 ± 10) is indicated by the
 175 yellow ‘sun’ in the center of the plot, near the average (123 ± 21) of the 6 (now 7) precursor
 176 methods that seem to be preferred. The overall average is 132 ± 47 (median 124). None of
 177 these numbers are substantially different, so one could perhaps just go with the “Wisdom of
 178 Crowds” (Aristotle, 350 BCE, “Politics”, III:xi; Galton, 1907).
 179

180 All predictions that we consider have the underlying assumption that the sun has not changed its
181 behavior (its “spots” so to speak) on a timescale of a few centuries (the Maunder Minimum may
182 be a possible violation of that assumption) and that there will be no such changes in the near
183 future, in spite of speculative suggestions like in Livingston et al. (2010) and Svalgaard (2013).

184 **Acknowledgments**

185 The author acknowledges the use of magnetic data from the Wilcox Solar Observatory
186 (<http://wso.stanford.edu/>), from Mount Wilson Observatory (<http://obs.astro.ucla.edu/intro.html>),
187 and of sunspot data from World Data Center-SILSO, Royal Observatory of Belgium, Brussels
188 (<http://www.sidc.be/silso/home>).

189 The author thanks Phil Scherrer at Stanford University for continued support and declares to
190 have no financial conflicts of interest.

191 **References**

192 Babcock, HW., Babcock, HD. 1955, The Sun’s magnetic field, 1952-1954. *The Astrophysical
193 Journal*, **121**: 349-366. <https://doi.org/10.1086/145994> .

194 Clette, F., Svalgaard, L., Vaquero, JM., Cliver, EW. 2014, Revisiting the Sunspot Number. A 400-
195 Year Perspective on the Solar Cycle. *Space Science Reviews* **186(1-4)**: 35-103.
196 <https://doi.org/10.1007/s11214-014-0074-2> .

197 Galton, F. 1907, Vox Populi. *Nature* **75(1949)**: 450-451. <http://doi.org/10.1038/075450a0> .

198 Hathaway, DH., Wilson, RM., Reichmann, EJ. 1994, The Shape of the Sunspot Cycle, *Solar
199 Physics* **151(1)**: 177-190. <https://doi.org/10.1007/BF00654090> .

200 Kitiashvili, IN. 2020, Application of Synoptic Magnetograms to Global Solar Activity Forecast.
201 *The Astrophysical Journal* **890(1)**: id.36, 1-29. <https://doi.org/10.3847/1538-4357/ab64e7> .

202 Livingston, W., Penn, MJ., Svalgaard, L. 2012, Decreasing Sunspot Magnetic Fields Explain
203 Unique 10.7 cm Radio Flux. *The Astrophysical Journal Letters* **757(1)**: L8.
204 <https://doi.org/10.1088/2041-8205/757/1/L8> .

205 McIntosh, SW., Chapman, SC., Leamon, RJ., Egeland, R., Watkins, NW. 2020, Overlapping
206 Magnetic Activity Cycles and the Sunspot Number: Forecasting Sunspot Cycle 25 Amplitude.
207 *Solar Physics* **xxx(x)**: xxx-xxx, temp: arXiv:2006.15263. <https://doi.org/10.1007/Bxxxxxxxxxx> .

208 NASA 2020, Solar Cycle 25 Is Here. <https://www.nasa.gov/press-release/solar-cycle-25-is-here-nasa-noaa-scientists-explain-what-that-means/> .

210 NOAA 2019, Solar experts predict the Sun’s activity in Solar Cycle 25 to be below average,
211 similar to Solar Cycle 24. <https://www.weather.gov/news/190504-sun-activity-in-solar-cycle> .

212 Pesnell, WD. 2016, Predictions of solar cycle 24: How are we doing? *Space Weather*, **14(1)**: 10-
213 <https://doi.org/10.1002/2015SW001304> .

214 Pesnell, WD. 2018, Effects of version 2 of the International Sunspot Number on naïve
215 predictions of Solar Cycle 25. *Space Weather*, **16(12)**: 1997-2003.
216 <https://doi.org/10.1029/2018SW002080> .

217 Pesnell, WD. 2020, How Well Can We Predict Solar Cycle 35? 2020 Sun-Climate Symposium,
218 Tucson, AZ, Jan. 2020.

219 https://lasp.colorado.edu/media/projects/SORCE/meetings/2020/final/S6_01_Pesnell_SunClimate.pdf .

- 220 Schatten, KH. 2005, Fair space weather for solar cycle 24. *Geophysical Research Letters*,
221 **32(21)**: L21106. <https://doi.org/10.1029/2005GL024363> .
- 222 Schatten, K. H., Scherrer, P. H., Svalgaard, L., Wilcox, J. M. 1978, Using Dynamo Theory to
223 predict the sunspot number during Solar Cycle 21. *Geophysical Research Letters* **5(5)**: 411-414.
224 <https://doi.org/10.1029/GL005i005p00411> .
- 225 Scherrer, PH., Wilcox, JM., Svalgaard, L. 1980, The rotation of the sun - Observations at
226 Stanford. *The Astrophysical Journal*, **241(1)**: 811-819. <https://doi.org/10.1086/158392> .
- 227 Shukuya, D., Kusano, K. 2017, Simulation Study of Hemispheric Phase-Asymmetry in the Solar
228 Cycle. *The Astrophysical Journal*, **835(1)**: id. 84. <https://doi.org/10.3847/1538-4357/835/1/84> .
- 229 Svalgaard, L. 2013, Solar activity - past, present, future. *Journal of Space Weather and Space
230 Climate* **3**: A24. <https://doi.org/10.1051/swsc/2013046> .
- 231 Svalgaard, L., Duvall Jr., TL., Scherrer, PH. 1978, The strength of the Sun's polar fields. *Solar
232 Physics* **58(2)**: 225-239. <https://doi.org/10.1007/BF00157268> .
- 233 Svalgaard, L., Cliver, EW., Kamide, Y. 2005, Sunspot cycle 24: Smallest cycle in 100 years?
234 *Geophysical Research Letters* **32(1)**: L01104. <https://doi.org/10.1029/2004GL021664> .
- 235 Svalgaard, L., Schatten, KH. 2008, Predicting Solar Cycle 24 (Using Solar Polar Fields). Invited
236 paper presented at the AGU Fall Meeting, San Francisco CA, Abstract SH51A-1593.
237 <https://leif.org/research/AGU-Fall-2008-SH51A-1593.pdf> .
- 238 Svalgaard, L., Kamide, Y. 2013, Asymmetric Solar Polar Field Reversals. *The Astrophysical
239 Journal* **763(1)**: id. 23. <https://doi.org/10.1088/0004-637X/763/1/23> .
- 240 Charbonneau, P. 2020, Dynamo models of the solar cycle. *Living Reviews of Solar Physics* **17**: 4-
241 104. <https://doi.org/10.1007/s41116-020-00025-6> .
- 242 Ulrich, RK., Evans, S., Boyden, JE., Webster, L. 2002, Mount Wilson synoptic magnetic fields:
243 Improved instrumentation, calibration, and analysis applied to the 2000 July 14 flare and to
244 evolution of the dipole field. *The Astrophysical Journal Supplement Series* **139(1)**: 259-279.
245 <https://doi.org/10.1086/337948> .
- 246 Waldmeier, M. 1955, *Ergebnisse und Probleme der Sonnenforschung*, 2nd edition. Akademische
247 Verlagsgesellschaft Geest & Portig, Leipzig, Germany.